Applied Physics A (2021) 127:541
https://doi.org/10.1007/s00339-021-04693-5

Applied Physics A
Materials Science & Processing

Nanopore creation in MoS_2 and graphene monolayers by nanoparticles impact: a reactive molecular dynamics study

Hamidreza Noori[1] · Bohayra Mortazavi[2] · Leila Keshtkari[3] · Xiaoying Zhuang[2] · Timon Rabczuk[1]

Received: 7 April 2021 / Accepted: 11 June 2021 / Published online: 20 June 2021

Abstract
In this work, extensive reactive molecular dynamics simulations are conducted to analyze the nanopore creation by nanoparticles impact over single-layer molybdenum disulfide (MoS_2) with 1T and 2H phases. We also compare the results with graphene monolayer. In our simulations, nanosheets are exposed to a spherical rigid carbon projectile with high initial velocities ranging from 2 to 23 km/s. Results for three different structures are compared to examine the most critical factors in the perforation and resistance force during the impact. To analyze the perforation and impact resistance, kinetic energy and displacement time history of the projectile as well as perforation resistance force of the projectile are investigated. Interestingly, although the elasticity module and tensile strength of the graphene are by almost five times higher than those of MoS_2, the results demonstrate that 1T and 2H-MoS_2 phases are more resistive to the impact loading and perforation than graphene. For the MoS_2nanosheets, we realize that the 2H phase is more resistant to impact loading than the 1T counterpart. Our reactive molecular dynamics results highlight that in addition to the strength and toughness, atomic structure is another crucial factor that can contribute substantially to impact resistance of 2D materials. The obtained results can be useful to guide the experimental setups for the nanopore creation in MoS_2or other 2D lattices.

Keywords MoS_2 · Graphene · Molecular dynamics · Impact · Nanopore

1 Introduction

Two-dimensional (2D) materials are crystalline materials consisting of a single layer of atoms. These materials have found applications in photovoltaic and photo-catalysts, semiconductors, electrodes and water purification [1, 2]. The extraordinary physical properties of 2D materials have the potential to both enhance existing technologies and also create a range of new applications. These materials can show exceptionally high mechanical [3], thermal [4] and electrical [5] as well as optical properties. These properties give them the ability to improve the performance of many products and materials. The 'enabling' characteristics of 2D materials allow them to either replace existing materials used in the manufacture of products or, in some cases, create completely new applications. One of the popular and very well-known 2D materials is graphene. Due to the extraordinary characteristics of graphene, it has attracted remarkable and increasing attentions of scientists in academia and industry as well. Outstanding strength resulting from strong covalent carbon-to-carbon bonds suggest graphene as unique candidate to enhance the mechanical properties of polymers. Graphene can also greatly improve the thermal conductivity of a material because of its exceptionally high thermal conductivity [6]. It is also very impermeable to both gasses and liquids [7, 8]. This property allows it to be exploited for a wide range of barrier applications. In applications which require very high electrical conductivity graphene can either be used by itself or as an additive to other materials [9, 10]. Even in very low concentrations, graphene can greatly enhance the ability of electrical charge to flow in a material [11]. Recently, numerous researches have been carried out to study the impact

✉ Bohayra Mortazavi
bohayra.mortazavi@gmail.com

✉ Timon Rabczuk
timon.rabczuk@uni-weimar.de

[1] Institute of Structural Mechanics, Bauhaus-Universität Weimar, Marienraße 15, 99423 Weimar, Germany

[2] Institute of Photonics, Department of Mathematics and Physics, Leibniz Universität Hannover, Appelstraße 11, 30167 Hannover, Germany

[3] Faculty of Mechanical and Materials Engineering, Graduate University of Advanced Technology, Kerman, Iran

behavior of graphene [12, 13] as well as resistance rupture and creation of nanopore in graphene [14–17]. The results demonstrate that graphene sheets can be used as bulletproofing due to its ultrahigh strength.

Another interesting and attractive 2D material is molybdenum disulfide (MoS_2). This material is classified as a transition metal dichalcogenides and is relatively nonreactive. This 2D material exists in semiconducting (2H), and metallic (1T) phases as are shown in Fig. 1. It is similar to graphite and has been widely used as a dry lubricant [18, 19] for several centuries because of its low friction and robustness and these days addressed among scientists for its appropriate properties. Single layer of molybdenum disulfide ($SLMoS_2$) can be mechanically exfoliated easily from its bulk counterpart [20], is a semiconducting analog to graphene [21], which shows an intrinsic band gap. It offers unique opportunities to tailor mechanical, thermal, electrical and optical properties as well as osmotic power generation [22–24]. A MoS_2 sheet consists of S_{top}-Mo-S_{bot} triple atomic planes, as shown in Fig. 1, with strong in-plane bonding. Interestingly depending on the arrangement of S atoms, $SLMoS_2$ of MoS_2 can exhibit contrasting electronic properties of semiconducting (2H) and metallic (1T) phases. Experimental achievements confirm the possibility of fabrication of MoS_2 hetero-structures made of semiconducting and metallic in a single-layer form. Due to experimental and theoretical estimations, MoS_2 is a material with a bright prospect for a wide variety of applications. Mechanical properties of semiconducting MoS_2 films have been studied both experimentally and theoretically [25–27].

The responses of the materials under high loading or impactare among the important engineering issues. Numerous experimental and theoretical simulations have been done to study the response of conventional and composite materials due to impact loading [28–30]. In addition, constructing a three-dimensional graphene structure [31] is performed to analyze the impact behavior of graphene sheets by ion beam irradiation. These studies reveal that graphene can demonstrate excellent energy dissipation during impact due to its full sp^2 strongly bonded carbon atoms. Haqueet et al. [12] studied impact behavior of graphene sheet using molecular dynamics simulations. In their study, one, two and three layers of graphene sheet were impacted with a fullerene rigid projectile in the impact velocity range of 3–8 km/s. In addition, Lee et al. [32] conducted 90 experiments to study the behavior of multilayer graphene membrane with the in-plane dimensions $L = W = 85$ μm and average thickness of 10–100 nm subjected to a spherical silica bullet with the mass of $m = 5.0 \pm 0.1 \times 10^{-14}$ kg. In their study at 600 m/s and 900 m/s impact velocities, post-impact analysis identifies three to six radial cracks initiating from the impact site with equal numbers of triangular-shaped petals creasing and folding at the base of the transverse cone which show graphene has extraordinary bullet resistance feature and excels in energy dissipation. Also, Avila et al. [33] have reported that addition of graphene sheets in the conventional composite materials increases their impact resistance. It was suggested that graphene sheets have advantages over carbon nanotubes (CNTs) since these are much easier to produce at relatively lower cost.

The investigations on 2D materials are extensive but still there is need for numerous studies. Researches show studies on one 2D material provide helpful understanding for the other family of 2D materials because many of the experimental set ups (initially for one 2D) can be used to perform measurements on other materials in this family. For example, the mechanical properties of single-layer MoS_2 ($SLMoS_2$) were successfully measured using the same nanoindentation platform as graphene [34, 35]. In the theoretical community, many theorems or approaches, which were initially developed to study graphene, are applicable to other quasi-two-dimensional materials. The interactions between the carbon atoms in graphene can be calculated using different computation levels: ab-initio density functional theory simulations and classical molecular dynamics simulations. For the modeling of MoS_2, there are various potentials available. Liang et al. [36] parameterized a bond-order potential for MoS_2, which was based on the bond-order concept underlying the Brenner potential [37]. Study the nanoindentation in MoS_2 thin films using a molecular statics approach [38], employing VFFM to calculate the phonon spectrum in bulk MoS_2 [39]. There are numerous theories and approaches are used to study graphene [40, 41], and later on, these approaches were considered to study MoS_2 [42, 43]. In these investigations, graphene and MoS_2 are compared and the results reveal in some applications graphene is more useful;

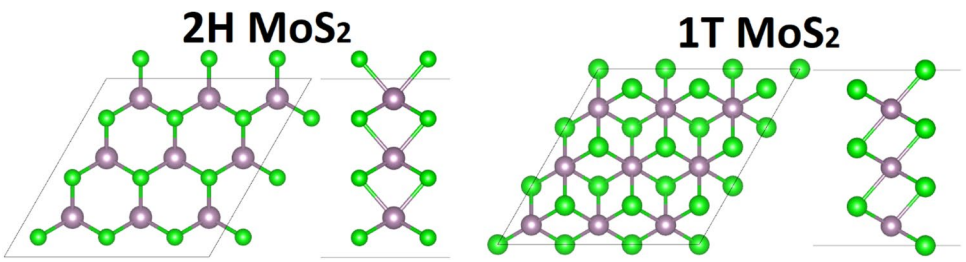

Fig. 1 Top and side views of 2H and 1T MoS_2 monolayers

however, there are some other applications that MoS_2 seems more competitive.

To date, numerous studies have been carried out to investigate the behavior of graphene impacted by high velocity projectile [33, 44, 45], and the results reveal graphene could be used as a high performance bulletproofing material. Researches on graphene versus MoS_2 have encouraged us to conduct molecular dynamics simulations on the impact of a projectile over three nanomembranes of graphene and MoS_2 with 1T and 2H phases. In order to conduct a direct comparison, the same conditions are considered for the three membranes. All the simulated membranes are with the same dimensions with fixed boundary conditions on the edges. Then, they are subjected to high velocity rigid projectile impacts the membranes at the center. Three different impact velocities are examined, and after the impact, different phenomena are observed. Projectile impacts the membrane and bounces back without breaking any bonds. Projectile impacts the membrane and some bonds are breaking, but the projectile does not pass through the membrane. Projectile bounces back or sticks to the target and then the whole system, membrane and projectile, vibrates. And finally, the minimum velocity that complete perforation happens is identified. Naturally, velocities higher than this velocity could break target bonds and passes through the target. Perforation, energy dissipation, and bullet trajectory are studied to identify the resistance of these three materials against high velocity impact. The results are compared and it will be discussed that how the strength and atomic structure of the nanosheet can contribute to the impact behavior.

2 Modeling

In the present study, Large-Scale Atomic/Molecular Massively Parallel Simulator (LAMMPS) [46] is used to carry out MD simulation; Open Visualization Tool (OVITO) [47] is used for the graphical presentations. The following process is employed, single-layer graphene (SLG) and single-layer MoS_2 with 1T ($SLMoS_2$-1T) and 2H ($SLMoS_2$-2H) sheets with the dimensions 200×200 nm as well as carbon sphere projectile with 20 nm diameter are constructed. The projectile coordinates introduced separately in each membrane file so that it hits the center of the target when it is allowed to move. An initial 6 Å distance is considered between the projectile and the target. As the main objective of this study is to find perforation and resistant force of the projectile, short distance initial position of the projectile does not affect the results but reduces the computational costs. All the nanomembranes edges, which are laid along x and y coordinate system directions, are fixed. The periodic boundary conditions considered in x and y planar directions, whereas along the z-direction non-periodic and shrink-wrapped (s) boundary condition is considered. The time step is used as 0.1 fs and the temperature is considered as 1 K to avoid thermal effect [12]. For the MoS_2 phases, the intra- and inter-molecular interactions are modeled by the ReaxFF [48] reactive potential, which is the best choice to predict mechanical behavior of MoS2 as discussed in the previous study [27]. Similarly the time step is used as 0.1 fs and the temperature is considered as 1 K to avoid thermal effect [12] like in case of graphene. Moreover, before fixing the edge atoms, sheets were relaxed by the Nosé-Hoover barostat and thermostat method at the desired temperature and to reach zero stress. Once the system was free of residual stresses, the structures were further equilibrated at 1 K temperature using Berendsen thermostat. Then, the atoms at boundaries were fixed; the simulations were carried out by giving different initial velocities to the projectile ranging from 2000 m/s to 15,000 m/s, 2000 m/s to 17,000 m/s, and 2000 m/s to 23,000 m/s for graphene, MoS_2-1T and MoS_2-2H, respectively. Three different velocity domains are identified to understand what happens to the target. With the low velocities, projectile moves toward the target, hits it, pushes the target in the same direction of velocity and then bounces back due to the elastic force of the stretched target. In these range of velocities, no bonds are broken. In the second range of velocities, the projectile moves toward the target, breaks some bonds and again bounces back or sticks to the target and vibrates with the target. In these velocities range, the number of breaking bonds depends on the values of initial velocity of the projectile, and such that a higher initial velocity leads to more breaking bonds. And finally, the third range of velocities is that the complete perforation happens. For these range and higher velocities, the projectile passes through the target after impact and a hole and cracks are created in the center of the target.

3 Results and discussions

We first study the impact behavior of single-layer graphene (SLG). Figure 2 shows the graphene and projectile structure before and during impact for different initial velocities. All the graphene edges are fixed and different initial velocities are applied to the projectile which moves toward the target along the sheet's normal direction and impacts the target. To examine the perforation, eight different initial velocities of 2000, 4000, 7000, 10,000, 11,000, 13,000, 14,000, and 15,000 m/s are applied to the projectile.

Figure 2 shows the target before and during impact. Figure 2a, b show the target before and after impact, respectively, with the projectile's velocity equal to 2000 m/s. In this velocity, the projectile impacts the target and bounces back as could be seen in Fig. 2b, and Fig. 2c and Fig. 2d show the projectile impacts the target for initial velocities

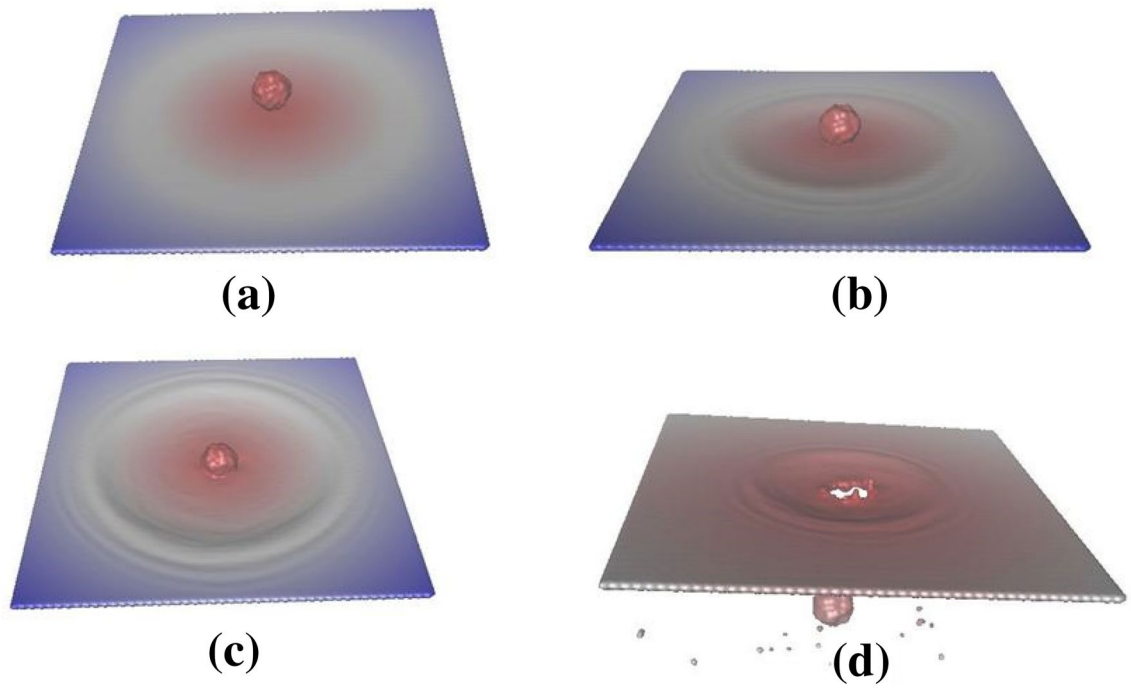

Fig. 2 **a** Single-layer graphene and the projectile before impact. **b** Projectile with initial velocity 2000 m/s impacts SLG and bounces back. **c** Projectile with initial velocity 7000 m/s impacts SLG and sticks to the target. **d** Projectile with initial velocity 11,000 m/s impacts SLG and complete perforation happens

equal to 7000 m/s and 11,000 m/s, respectively. When the velocity is 7000 m/s, some bonds are broken and projectile penetrates through the target and the whole system vibrates. In the case of projectile's velocity equal to 11,000 m/s, the complete perforation happens and then projectile continues to moves in negative z-direction. Generally, three cases happen and change in projectile's kinetic energy and displacement versus time are plotted in Fig. 3. In the first case, the projectile's initial velocities are lower than 5000 m/s and there is no enough kinetic energy to break bonds of the graphene layer. As shown in Fig. 2b, for example, when the initial velocity equal to 2000 m/s, the projectile hits the graphene, pushes the graphene and reaches maximum displacement in the negative z-direction, stops for an instant that at this time it has zero kinetic energy. The stretched graphene causes the bullet bounces back with lower kinetic energy than its initial kinetic energy and a harmonic circular wave is created, similar a wave appears by throwing a stone inside immovable and stationary water, and propagates through the target. The wave starts from the center, travels through the target and transmits energy, reaches the boundaries and finally the wave and its energy reflected back. Also, by considering Fig. 3, it can be seen that the change of kinetic energy and displacement versus time for initial velocity equal to 2000 m/s. Kinetic energy is constant as the bullet travels through the initial gap and then decreases during impact, turn to zero when reaches the maximum displacement. Then, the bullet bounces back due to the elastic force of the stretched target and the kinetic energy starts to increases but not considerably and finally remains constant. The displacement of the projectile versus time for initial velocity equal to 2000 m/s is shown in Fig. 3. It can be seen the projectile travels toward the target and pushes it in the negative z-direction and reaches the maximum displacement. Then bounces back due to the elastic force of the target and continues to travel in positive z-direction. For the velocities between 4000 to 5000 m/s, as it can be seen in Fig. 3 where initial velocity equal to 4000 m/s, the projectile impacts the graphene, no breaking of bonds happen, but does not bounces back similar to that happened when the initial velocity is equal to 2000 m/s. In the aforementioned range of velocities, the projectile impacts the target, pushes it back in the negative z-direction, sticks to the target and for a moment the projectile's velocity becomes zero. The stretched graphene pushes the projectile back and all the system vibrates together. Similar to that happened for the velocity equal to 2000 m/s a harmonic circular wave is created in the center of graphene, moves to the boundaries and reflected back.

In the second case, the projectile's initial velocities are between 5500 and 10,000 m/s. In these range of speeds, the projectile starts to break some graphene's bonds, but the

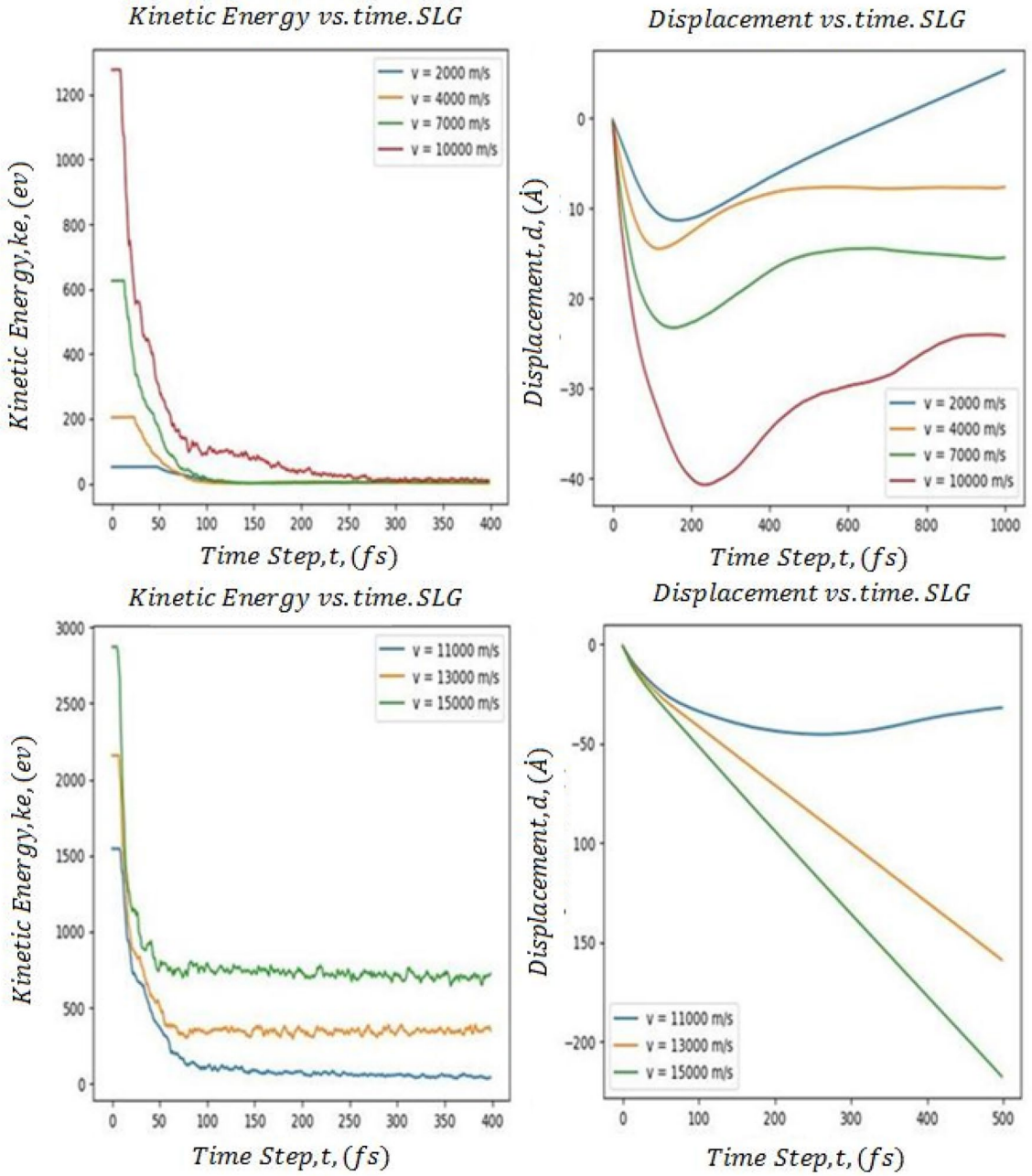

Fig. 3 Change of projectile's kinetic energy and displacement versus time for different range of impact velocities over single-layer graphene (SLG)

complete perforation does not happen. After breaking some bonds, the projectile sticks to the graphene layer and all the system vibrates together. The number of breaking bonds depends on the initial velocity of the projectile. Higher initial velocities break more bonds. Similar to the first case, the wave is created in the center of target and propagates through the target, transmits energy, reaches the boundaries and finally the wave and its energy reflected back. In the last case, the projectile's initial velocities are more than 10,500 m/s. In this case, the projectile completely passes through the graphene layer and complete perforation happens. The projectile loses some of its kinetic energy, passes through the graphene, and with constant kinetic energy continues to move in the negative z-direction. Similar to 1st case and 2nd case, the wave and its energy move through the target and reflected back as reaches the boundaries. The amount of projectile's kinetic energy after complete perforation depends on the value of the initial velocity as it could

be seen in Fig. 3. For initial velocity equal to 13,000 m/s, the projectile leaves the target with the kinetic energy equal to nearly 250 eV; however, for the initial velocity equal to 15,000 m/s, the kinetic energy is nearly equal to 1300 eV after perforation. It should be mentioned that our predicted velocities are relatively high compared to those numerical results [12] in which complete perforation happens at 4500 m/s for single-layer graphene. In the study by [12], mass of the projectile consists of 180 carbon atoms which is lower than the present study in which projectile's mass consists of 207 carbon atoms. This should results in the present study perforation has to take place in lower velocities than those obtained by [12]. However, the mass is not the only factor that contributes to the impact problems.

The size of the projectile shows a significant effect on the impact loading problems. In the previous study [12], the projectile's diameter is 12 Å which is nearly two times smaller than the projectile's diameter in the present study (20 Å). As the projectile's diameter increases, the contact surface increases; therefore, more initial velocity is needed for the complete perforation. This could be approved by the following formulation that demonstrates the movements of a projectile through a media. When a moving object passes through a media, it experiences resistive forces via the media. In general, the resistive force could be written as follows:

$$F_{\text{res}} = -\left(k_1 v + k_2 v^2\right)\hat{v} \tag{1}$$

In Eq. (1), the first term in the right-hand side is called viscous term and the second one is called pressure term. $\hat{v}$ is unite vector and the minus sign states the resistive force is in the opposite direction of the speed. Furthermore, the resistive force applied on the bullet is represented by k_1, and k_2 which are depend on the kind of medium that the bullet passes through. Generally, the resistive force depends on the shape of the object, the size of the object, the medium that objects movingthrough, and the speed of the object. In this paper, the object is considered to be a sphere and consequently the magnitude of the resistance force in the Eq. (1) can be written as:

$$\left|F_{\text{res}}\right| = c_1 r v + c_2 r^2 v^2 \tag{2}$$

where c_1 and c_2 are constant with the dimensions of $\frac{\text{kg}}{\text{m s}}$ and $\frac{\text{kg}}{\text{m}^3}$, respectively. Equation (2) shows the resistance force which results in how the target can resists against the projectile, which strongly depends on the radius of the projectile. This is the reason why in the present study, the perforation happens in higher velocities than those reported in [12]. In order to conduct a numerical validation, a model similar to that one in earlier study [12] was conducted, with single-layer graphene with the dimensions of 200 × 200 Å and a projectile with a radius of 12 Åwith the same mass. The complete perforation happens for the initial velocities higher than 5000 m/s, which is in a close agreement with the results in the work by [12], that suggests the perforation happens for the initial velocities higher than 4500 m/s. Also, a model constructed similar to that experimented by [32], (projectile with the mass $m = 3.61 \times 10^{-24}$ kg) and complete perforation happened at the minimum velocity equal to 630 m/s which is in a good agreement by the value of 600 m/s reported experimentally [32]. It should be mentioned that the velocity of conventional bullets is in the range of 1000–2000 m/s. In our theoretical analysis, we found the velocities that the projectile's impact can result in the rupture of the graphene are very high. Nonetheless, if we have used bullet with bigger mass, the rupture would occur at lower velocities. This way, our results like other theoretical simulations can be useful to comparatively study the impact problems, rather than concentrating on the absolute values of the projectile's velocity. We next explore the impact behavior of single-layer graphene MoS2 with 1T phase (MoS2-1T). Like graphene elaborately discussed above, a MoS2-1T sheet with 200 × 200 nm along x and y-directions subjected to a 20 nm carbon projectile that initially distanced 6 Å from the target's center in z-direction. As stated before, ReaxFF thoroughly is used in many studies to model intra- and inter-molecular interactions in graphene and MoS_2. These studies demonstrated taht ReaxFF and AIREBO force field reasonably predicted the mechanical behavior of MoS_2 and graphene. Therefore, in this study, ReaxFF potential is employed to predict the transverse impact behavior of MoS_2 subjected to a high velocity carbon projectile. The graphical view of MoS2-1T and projectile before and after impact is shown in Fig. 4. Figure 4a shows the whole structure, including projectile and target, before impact. Figure 4b, c show the impact for the initial velocities equal to 2000 and 7000 m/s, respectively. For the velocity equal to 2000 m/s, the bullet impacts the target, presses the sulfide bonds and then bounces back. The compression of sulfide bonds which are bonded to molybdenum atoms in the middle leads to distortion in the target. Unlike the case of graphene, a circular wave is not created and the distortion resembles that of the higher modes of vibration. As the projectile reaches maximum distance, bounces back due to the force of compressed bonds connected to the sulfide atoms and also due to the stretched middle layer. When the velocity is equal to 7000 m/s as shown in Fig. 4c, the projectile hits the target, but does not bounces back. In this velocity, the projectile sticks to the target and vibrates with the target. Like the previous impact, the target distorted as if higher vibration modes are created.

As expected, higher velocities lead to more distortion and creation of higher vibration modes. The Fig. 4d shows the complete perforation for the initial velocity equal to 17,000 m/s. In this velocity, the projectile hits the target

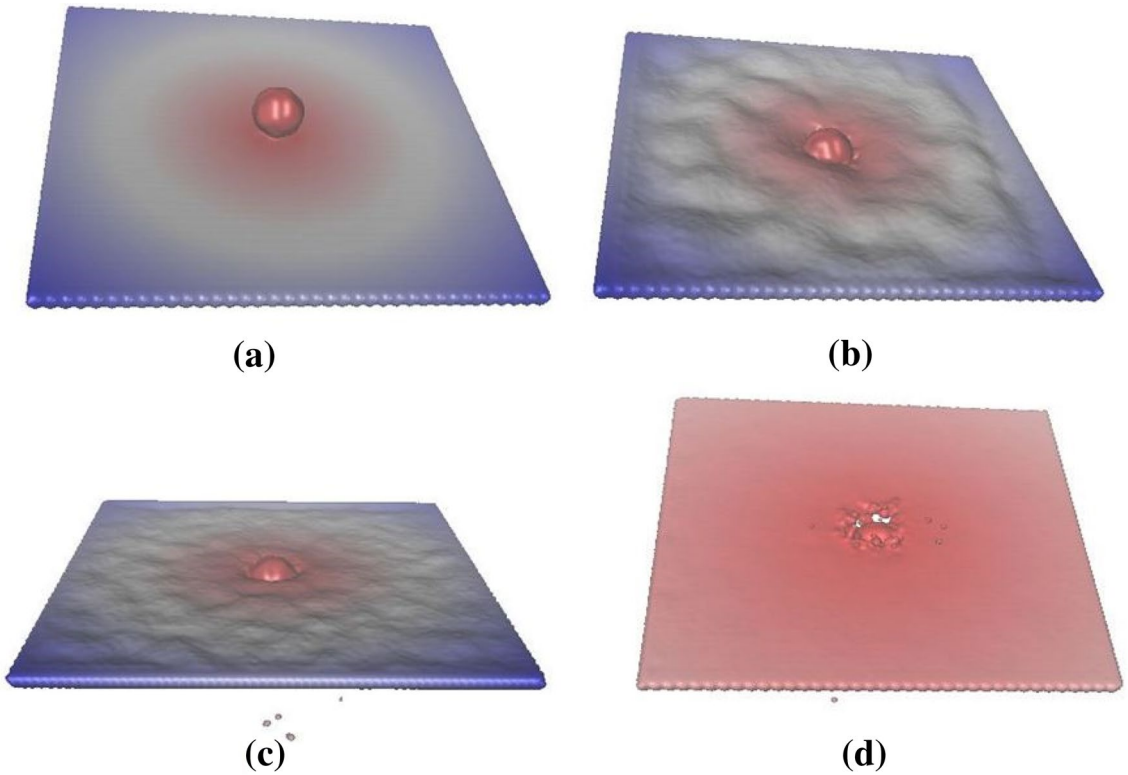

Fig. 4 $SLMoS_2$-1T and projectile's structure before impact. **b** Projectile with the initial velocity of 2000 m/s impacts $SLMoS_2$-1T and bounces back. **c** Projectile with the initial velocity of 7000 m/s impacts the sheet and sticks to the target. **d** Projectile with the initial velocity of 17,000 m/s impacts and complete perforation happens

and passes through the target. The higher velocities lead to higher modes of vibration and more distortion. To examine the perforation, different initial velocities equal to 2000, 7000, 10,000, 13,000, 14,000, 15,000, 17,000 m/s are applied to the projectile. The change of projectile's kinetic energy and displacement versus time are plotted in Fig. 5 for different initial velocities. As a constant routine, three different cases happen: in the 1st case, the initial velocity is lower than 3000 m/s. In these range of velocities, there are no braking bonds. The projectile impacts the MoS_2-1T sheet, presses the sulfide connected bounds to molybdenum and creates some distortion in the target like standing waves and finally bounces back due to the elastic force of the connected bonds and stretched middle plane. When the projectile hits the target loses most of its kinetic energy and bounces back with a small amount of kinetic energy. The converted energy turns into potential energy in the target, heat, and other form of energy. Unlike the graphene, it seems that waves do not move, just distortion happens in the target like higher modes of vibration. In the 2nd case, the applied initial velocities are between 3000 and 13,000 m/s. In this extension of velocities, the projectile impacts the target, breaks some bonds and adheres to the target. The projectile loses all of its kinetic energy which converted to the potential energy in the target, heat, and other form of energy. The number of breaking bonds depends on the initial velocity of the projectile, and it means bigger initial velocities lead to more breaking bonds. Also, higher velocity results in higher vibration modes happen in the target. This happening higher modes and distortion lead to not only the breaking bonds happen in the area of impact, but also some bonds far from the impact area will break. In the last and 3rd case, the velocities are more than 14,000 m/s. In this case, the projectile hits the target and passes through the target and complete perforation happens. After perforation, the projectile continues to move with a constant velocity which is much less than initial velocity due to the loss of kinetic energy. Like the 2nd case, higher vibration modes created in the target and distort the target. As mentioned, braking of bonds are not just in the impact area but also in the other parts of the target. As the initial velocity increases and are very high, the distortion increases and the breaking of bonds happen at regions farer from the impact location.

Last but not least, we study the impact over single-layer MoS_2-2H sheet. Different initial velocities equal to 2000, 4000, 10,000, 13,000, 17,000, 19,000, 23,000 m/s are given

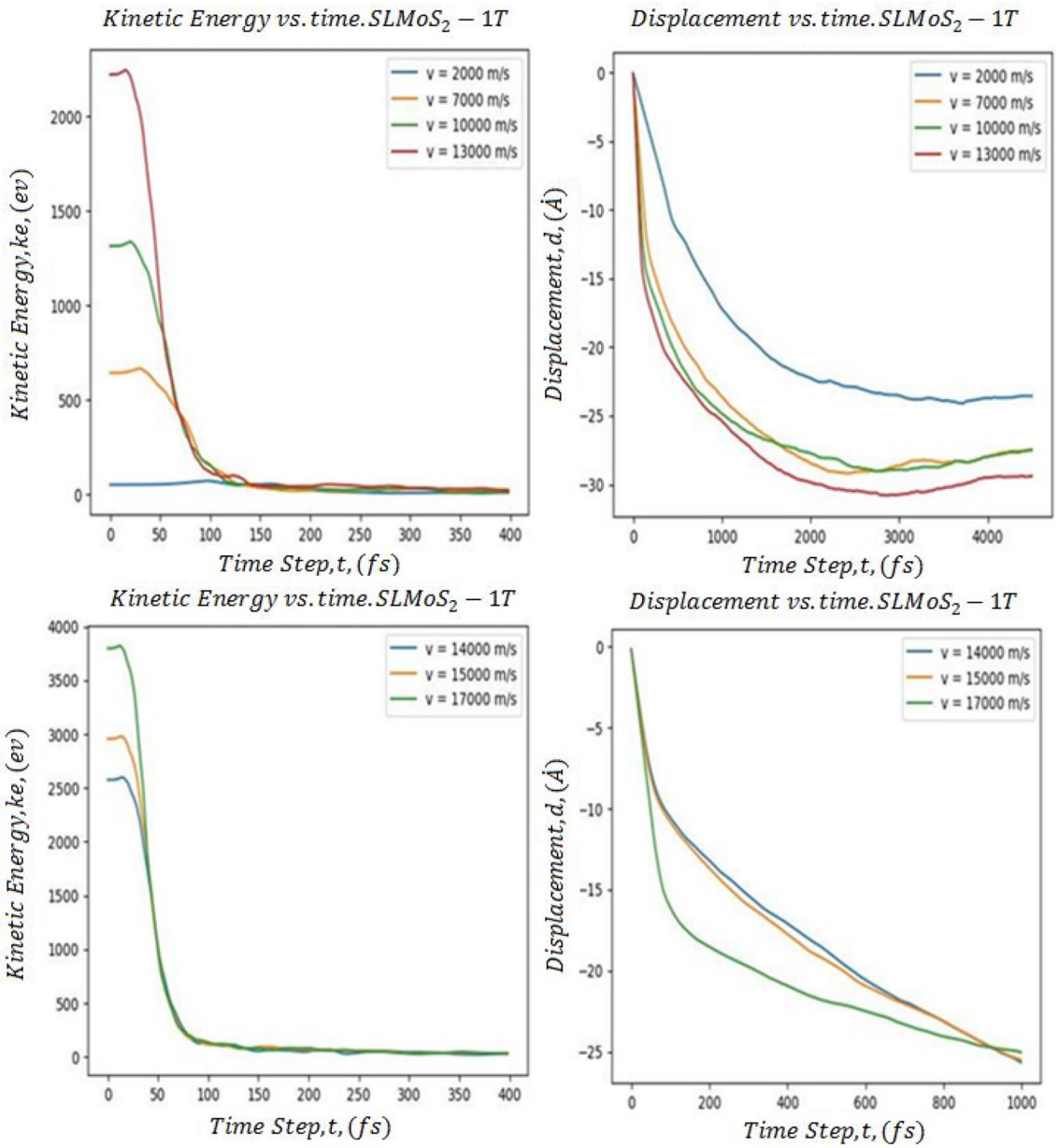

Fig. 5 Change of projectile's kinetic energy and displacement versus time for different range of velocities, $SLMoS_2$-1T

to the projectile. The pictorial appreciation of the impact is shown in Fig. 6. Figure 6a shows the whole system before impact where the target is completely flat and the projectile distanced 6 Å from the target. Figure 6b represents the impact with initial velocity equal to 2000 m/s. With this initial velocity, projectile impacts the target and creates a circular wave in the center which propagates through the target. The wave transmits the energy and reaches the boundaries and then reflects back toward the center. The wave's velocity is considerably less than in the case of graphene. The projectile compresses the sulfide bonds that are bonded to the molybdenum atoms in the middle plane and then pushes the target. As the projectile reaches the maximum displacement, bounces back due to the elastic force of the stretched middle plane and the compression force of the sulfide-molybdenum bonds.

Figure 6c represents pictorial view of the impact when the initial velocity is equal to 7000 m/s. In this velocity, the projectile impacts the target and compresses the sulfide bonds which are connected to the molybdenum atoms and pushes the target in the negative z-direction. The projectile breaks some bonds and adheres to the target. A circular wave creates in the center of the target and propagates through the target, reaches the boundaries and reflected back. The

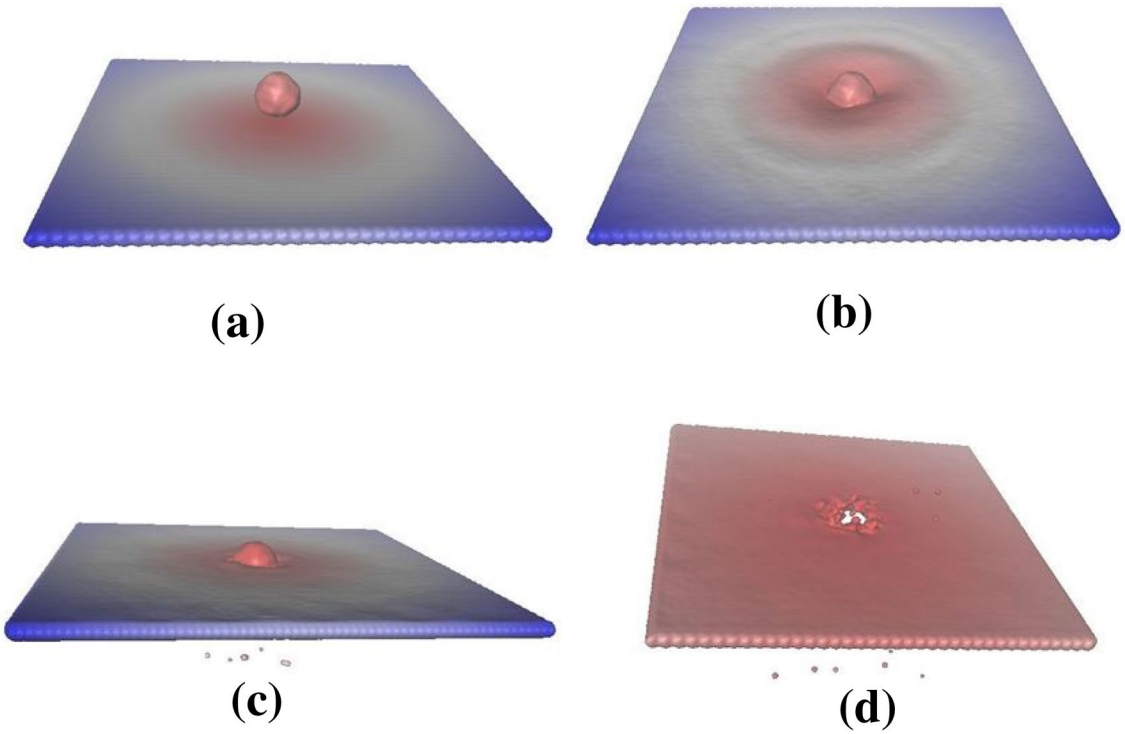

Fig. 6 **a** $SLMoS_2$-2H and projectile's structure before impact. **b** Projectile with initial velocity 2000 m/s impacts $SLMoS_2$-2H and bounces back. **c** Projectile with initial velocity 7000 m/s impacts the sheet and sticks to the target. **d** Projectile with initial velocity 23,000 m/s impacts and complete perforation happens

reflected wave transmits the energy and causes the vibration of the target and the projectile. Figure 6d shows the impact when the initial velocity is equal to 23,000 m/s. In this velocity, the projectile hits the target and passes through the target and complete perforation happens. A circular wave created in the center of the target and propagates through the target and reflected back as reaches the boundaries. Similar to that happens to graphene and MoS_2-1T, three different cases occur and graphical view of changing in projectile's displacement and kinetic energy versus time is presented in Fig. 7 for different initial velocity of the projectile. In the 1st case, velocities are less than 4000 m/s that leads to no breaking bond. The projectile impacts the target, compress the connected bonds of sulfide to molybdenum and pushes the target, loses all of its kinetic energy and stops for a moment at maximum displacement, and finally bounces back due to the elastic force of the stretched target and compressed bonds with much less kinetic energy than initial kinetic energy. As aforementioned, projectile's kinetic energy converts to potential energy of the target, heat, and other form of energy. The 2nd case is related to velocities between 4000 and 19,000 m/s. In this case, some bonds are broken and the projectile adheres to the target. Perforation does not happen, and the projectile and the target vibrate due to the transmitted and reflected wave. The number of breaking bonds depends on the values of the initial velocity, and for higher initial velocity, more bonds break. In the 3rd case, the velocities are higher than 19,000 m/s and the complete perforation happens. The projectile impacts the target, breaks bonds and passes through the target. Most of projectile's kinetic energy converts to the other form of energy and as the projectile passes through the target, continues to move with constant kinetic energy.

Figure 8 shows the time history of the perforation resistance force for SLG. Initially, as long as the projectile travels in vacuum, resistance force is zero. When the projectile starts to contact with the target, resistance force starts to increase. After reaching a maximum value, force starts to decreases with time. Peak value of the resistance force increases with the impact velocity. These perforation resistance forces are higher than the perforation resistance force those are presented by [12] for SLG for the same initial velocity. In their study, it is stated that the resistance force increases with the impact velocity and number of graphene sheets. In our study for the initial velocity equal to 7000 m/s, the maximum value of the resistance force is virtually 230 nN for SLG, which is nearly the same as the value reported by [12] for bi-layers graphene sheet (2L-GS). The reason for higher

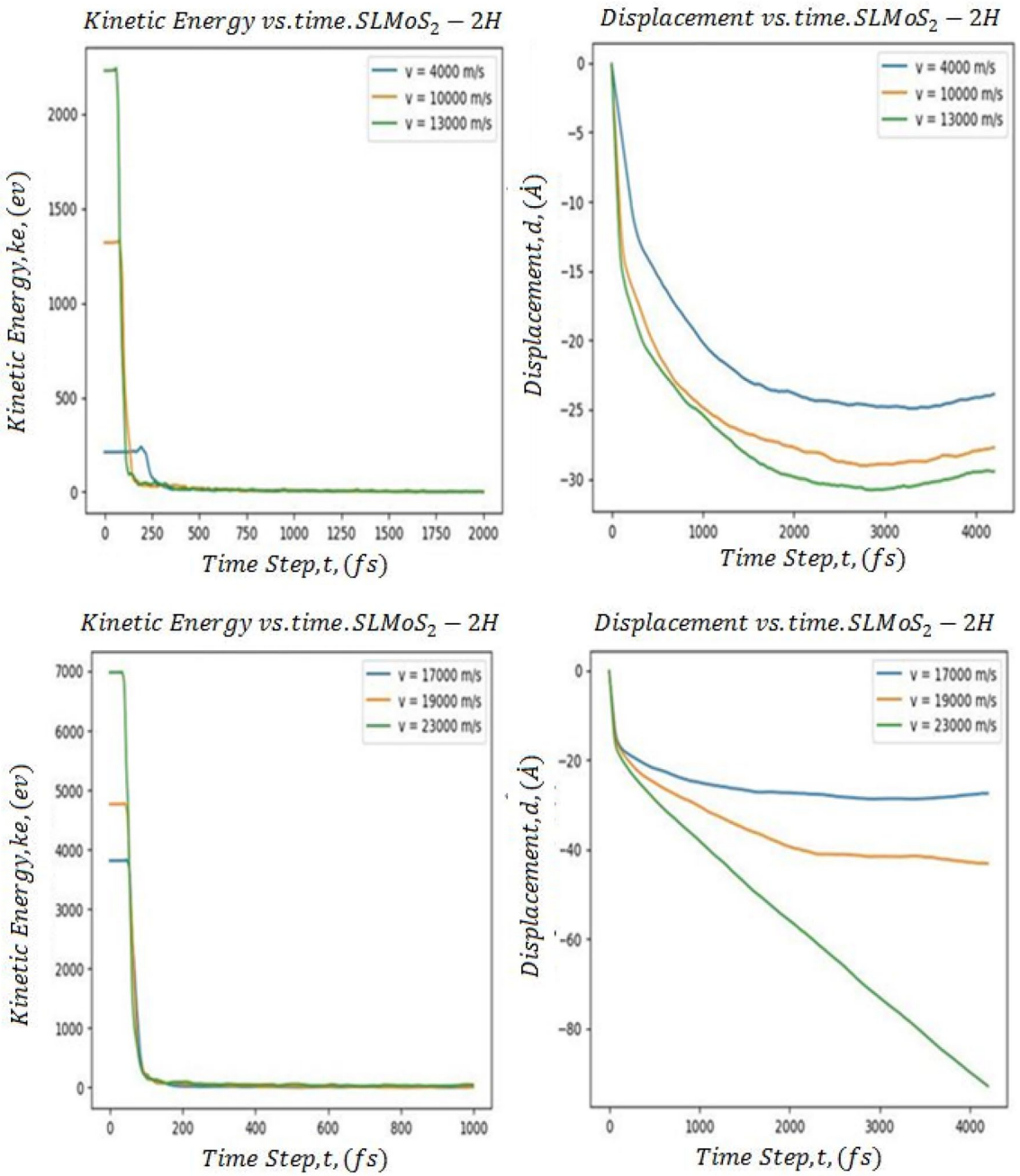

Fig. 7 Change of projectile's kinetic energy and displacement versus time for different range of velocities, $SLMoS_2$-2H

resistance force compare to [12] is that in the present study, the diameter of the projectile is nearly two times bigger than the projectile's diameter in the earlier study [12]. As stated before and theoretically confirmed by the Eqs. 1 and 2, the increase in projectile's diameter leads to increase in contact surface during impact and results in higher resistance force.

The time history of the perforation resistance force for $SLMoS_2$-1T is presented in Fig. 9. As long as the projectile travels through the vacuum to reach the monolayer, the resistance force is zero. The resistance force starts to increase as soon as the impact occurs. Resistance force increases during impact and reaching a maximum value and then begins to decrease. As expected, the peak of the resistance force increases with the impact velocity. Figure 9 also shows impact resistance force for $SLMoS_2$-2H. Worthy to note according to earlier MD study, 2H phase of MoS_2 nanosheet is considerably stronger than its 1T counterpart [27], which is consistent with our reported results

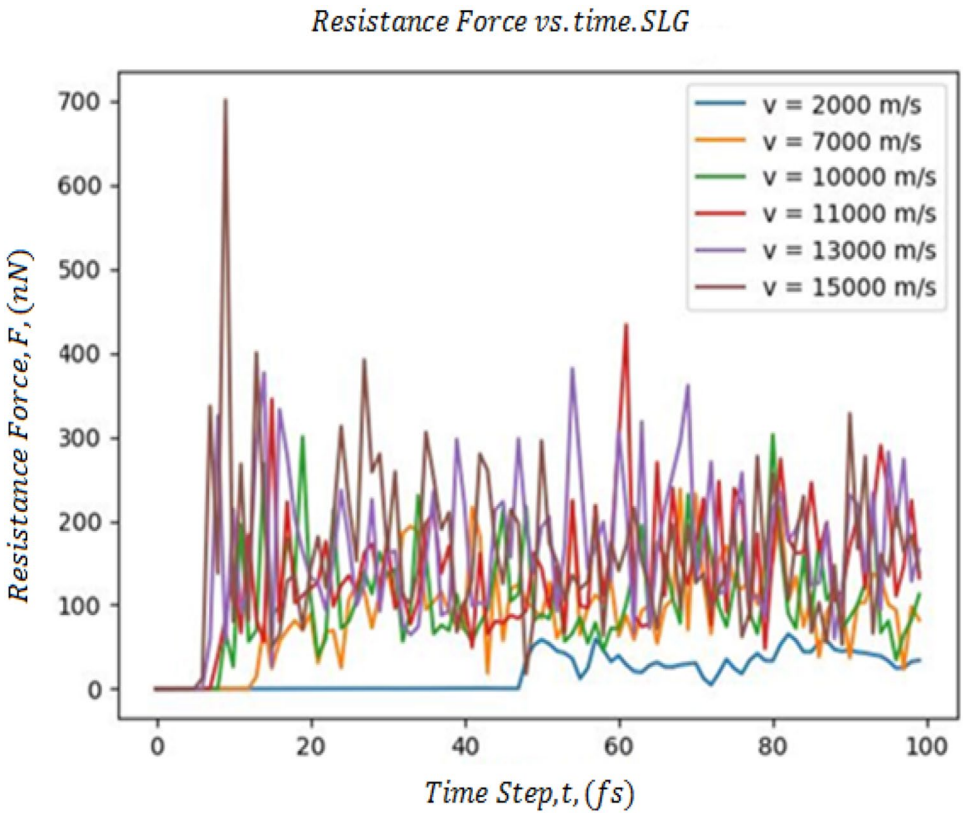

Fig. 8 Perforation resistance force versus time for single-layer graphene

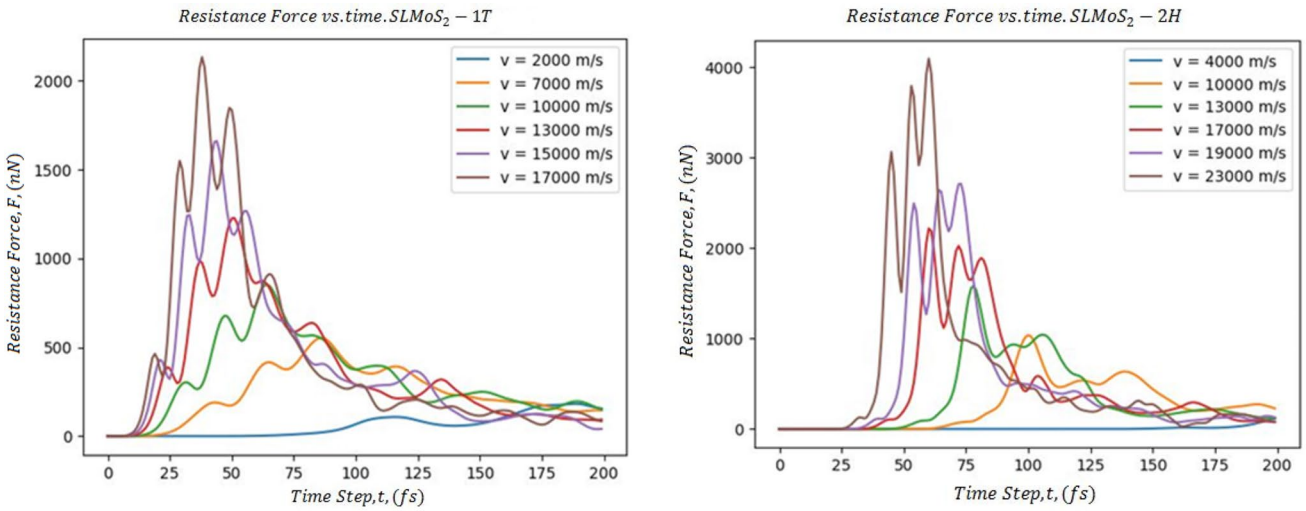

Fig. 9 Perforation resistance force versus simulation time for $SLMoS_2$-1T and $SLMoS_2$-2H

which indicate higher resistive forces for the impact over $SLMoS_2$-2H than $SLMoS_2$-1T. By comparing the results shown in Figs. 8 and 9, it is clear that the maximum resistance force is highest for $SLMoS_2$-2H and minimum for the SLG.

To summarize our results, we have conducted the simulations with initial impact velocities of 2000, 7000, 10,000, 13,000, 14,000, 15,000 and 17,000 m/s. We predicted that for the SLG, perforation happens for the initial velocities more than 10,000 m/s. For the $SLMoS_2$-1T and $SLMoS_2$-2H, the perforation happens for the velocities more than 14,000 m/s and 19,000 m/s, respectively. It is thus clear that required energy for the nanopore creation in MoS_2 monolayers is considerably higher than SLG, which is a very interesting finding. Lee et al. [32] realized that the combination of strength and toughness of a material are two important

factors that contribute to stop speeding projectile as well as dissipating the absorbed kinetic energy. In their study, they found specific penetration energy for multilayer graphene is virtually 10 times more than the literature value for macroscopic steel sheet at 600 m/s. Although the breaking strength and young's modules of SLG are nearly 5 times more than the $SLMoS_2$ [26], the penetration happens with smaller kinetic energy for graphene compare to $SLMoS_2$ phases. In the present study, as a new fining, we show that in addition to the strength and toughness, there are other factors that can contribute to improve bulletproofing application. With our reactive molecular dynamics results, we clearly show that atomic structure can yield substantial enhancement in bulletproofing. The superiority of MoS_2 to graphene can be attributed to its layered structure, in which a plane of molybdenum atoms is sandwiched by planes of sulfide atoms (S_{top}–Mo–S_{Bot}) as shown in Fig. 1. In this system, strong in-plane bonding forms between Mo and S atoms. In this simulation, we understood that topology and atomic configuration of the material play important role in impact problems. The 2H phase is the original structure of MoS_2 which shows a hexagonal lattice with the atomic stacking sequence of ABA. On the other hand, 1T phase represents an atomic stacking sequence of ABC, in which the S atoms on the bottom are placed in the hollow center of the hexagonal lattice. In accordance with the results shown in earlier theoretical simulations [27], the arrangement of sulfide atoms in two phases also changes the mechanical strength and contributes to amplify the perforation resistance and energy absorption during impact.

4 Conclusion

Extensive reactive molecular dynamics simulations are performed to estimate resistance of single-layer graphene, MoS_2-1T and MoS_2-2H to the impact loading. As a remarkable finding, we show that despite the higher strength and toughness of graphene compare to MoS_2 monolayer, MoS_2 shows distinctly higher resistance to the impact loading as compared to graphene. The underlying mechanism is discussed to be due to the three-layered sandwich structure of MoS_2 phases. Our results also indicate higher resistive forces for the impact over 2H phase of MoS_2 than its 1T lattice. Therefore, it could be concluded that in addition to the strength and toughness, atomic structure is another crucial factor that can contribute substantially to impact resistance of 2D materials. Outcomes of this study can also guide the experimental studies for the nanopore creation in MoS_2 nanosheets.

Acknowledgements B.M. and X.Z. appreciate the funding by the Deutsche Forschungsgemeinschaft (DFG, German Research Foundation) under Germany's Excellence Strategy within the Cluster of Excellence PhoenixD (EXC 2122, Project ID 390833453). Authors are greatly thankful to the VEGAS cluster at Bauhaus University of Weimar for providing the computational resources.

Funding Open Access funding enabled and organized by Projekt DEAL.

References

1. W. Li, Y. Yang, J.K. Weber, G. Zhang, R. Zhou, Tunable, strain-controlled nanoporous MoS2 filter for water desalination. ACS Nano **10**, 1829–1835 (2016)
2. K. Rasool et al., Water treatment and environmental remediation applications of two-dimensional metal carbides (MXenes). Mater. Today **30**, 80–102 (2019)
3. J.H. Kim, J.H. Jeong, N. Kim, R. Joshi, G.-H. Lee, Mechanical properties of two-dimensional materials and their applications. J. Phys. D. Appl. Phys. **52**, 83001 (2018)
4. X. Gu, Y. Wei, X. Yin, B. Li, R. Yang, Colloquium: phononic thermal properties of two-dimensional materials. Rev. Mod. Phys. **90**, 41002 (2018)
5. M. Salavati, Electronic and mechanical responses of two-dimensional HfS2, HfSe2, ZrS2, and ZrSe2 from first-principles. Front. Struct. Civ. Eng. (2018). https://doi.org/10.1007/s11709-018-0491-5
6. Y. Fu et al., Graphene related materials for thermal management. 2D Mater. **7**, 12001 (2019)
7. V. Berry, Impermeability of graphene and its applications. Carbon N. Y. **62**, 1–10 (2013)
8. J.S. Bunch et al., Impermeable atomic membranes from graphene sheets. Nano Lett. **8**, 2458–2462 (2008)
9. Y. Li et al., Additive manufacturing high performance graphene-based composites: a review. Compos. Part A Appl. Sci. Manuf. **124**, 105483 (2019)
10. D. Schmeltzer, A. Saxena, Superconductivity in graphene induced by the rotated layer. J. Phys. Condens. Matter **32**, 475603 (2020)
11. B. Yuan et al., Electrical conductive and graphitizable polymer nanofibers grafted on graphene nanosheets: Improving electrical conductivity and flame retardancy of polypropylene. Compos. A Appl. Sci. Manuf. **84**, 76–86 (2016)
12. Haque, B. Z. (Gama), Chowdhury, S. C. & Gillespie, J. W. Molecular simulations of stress wave propagation and perforation of graphene sheets under transverse impact. *Carbon N. Y.* **102**, 126–140 (2016).
13. M. Salavati, N. Alajlan, T. Rabczuk, Super-stretchability in two-dimensional RuCl3 and RuBr 3 confirmed by first-principles simulations. Phys. E Low-Dimensional Syst. Nanostruct. **113**, 79–85 (2019)

14. S. Sadeghzadeh, Benchmarking the penetration-resistance efficiency of multilayer graphene sheets due to spacing the graphene layers. Appl. Phys. A **122**, 655 (2016)
15. S. Sadeghzadeh, Computational design of graphene sheets for withstanding the impact of ultrafast projectiles. J. Mol. Graph. Model. **70**, 196–211 (2016)
16. S. Sadeghzadeh, Geometric effects on nanopore creation in graphene and on the impact-withstanding efficiency of graphene nanosheets. Mech. Adv. Compos. Struct. **5**, 91–102 (2018)
17. S. Sadeghzadeh, L. Liu, Resistance and rupture analysis of single- and few-layer graphene nanosheets impacted by various projectiles. Superlattices Microstruct. **97**, 617–629 (2016)
18. C. Donnet, A. Erdemir, Historical developments and new trends in tribological and solid lubricant coatings. Surf. Coatings Technol. **180–181**, 76–84 (2004)
19. C. Donnet, J.M. Martin, T. Le Mogne, M. Belin, Super-low friction of MoS2 coatings in various environments. Tribol. Int. **29**, 123–128 (1996)
20. G.S. Papanai, I. Sharma, G. Kedawat, B.K. Gupta, Qualitative analysis of mechanically exfoliated MoS2 nanosheets using spectroscopic probes. J. Phys. Chem. C **123**, 27264–27271 (2019)
21. A. Castellanos-Gomez et al., Laser-thinning of MoS2: on demand generation of a single-layer semiconductor. Nano Lett. **12**, 3187–3192 (2012)
22. M. Salavati, A. Mojahedin, A.H.N. Shirazi, Mechanical responses of pristine and defective hexagonal boron-nitride nanosheets: a molecular dynamics investigation. Front. Struct. Civ. Eng. **14**, 623–631 (2020)
23. M. Tabatabaeichehr, H. Mortazavi, The effectiveness of aromatherapy in the management of labor pain and anxiety. Ethiop. J. Health Sci. **30**, 449–458 (2020)
24. F. Rahimi Mehr, M. Salavati, A. Morgenthal, S. Kamrani, C. Fleck, Computational analysis and experimental calibration of cold isostatic compaction of Mg-SiC nanocomposite powders. Mater. Today Commun. **27**, 102321 (2021)
25. S. Bertolazzi, J. Brivio, A. Kis, Stretching and breaking of ultrathin MoS2. ACS Nano **5**, 9703–9709 (2011)
26. H.R. Noori, E. Jomehzadeh, N. Alajlan, T. Rabczuk, Elastic deformation behavior of freestanding MoS2 films using a continuum approach. Solid State Commun. **280**, 24–31 (2018)
27. B. Mortazavi, A. Ostadhossein, T. Rabczuk, A.C.T. van Duin, Mechanical response of all-MoS2 single-layer heterostructures: a ReaxFF investigation. Phys. Chem. Chem. Phys. **18**, 23695–23701 (2016)
28. B.A. Gama et al., High strain-rate behavior of plain-weave S-2 glass/vinyl ester composites. J. Compos. Mater. **35**, 1201–1228 (2001)
29. J.W. Gillespie Jr., A.M. Monib, L.A. Carlsson, Damage tolerance of thick-section S-2 glass fabric composites subjected to ballistic impact loading. J. Compos. Mater. **37**, 2131–2147 (2003)
30. T. El Sayed, W. Mock, A. Mota, F. Fraternali, M. Ortiz, Computational assessment of ballistic impact on a high strength structural steel/polyurea composite plate. Comput. Mech. **43**, 525–534 (2009)
31. M.A. Abdol, S. Sadeghzadeh, M. Jalaly, M.M. Khatibi, Constructing a three-dimensional graphene structure via bonding layers by ion beam irradiation. Sci. Rep. **9**, 8127 (2019)
32. J.-H. Lee, P.E. Loya, J. Lou, E.L. Thomas, Dynamic mechanical behavior of multilayer graphene via supersonic projectile penetration. Science (80-) **346**, 1092LP – 1096 (2014)
33. A.F. Ávila, A.S. Neto, H. Nascimento Junior, Hybrid nanocomposites for mid-range ballistic protection. Int. J. Impact Eng. **38**, 669–676 (2011)
34. Cooper, R. *et al.* Nonlinear elastic behavior of two-dimensional molybdenum disulfide. *Phys. Rev. B* **87** (2013).
35. C. Lee, X. Wei, J.W. Kysar, J. Hone, Measurement of the elastic properties and intrinsic strength of monolayer graphene. Science (80-) **321**, 385LP – 388 (2008)
36. Liang, T., Phillpot, S. R. & Sinnott, S. B. Parametrization of a reactive many-body potential for Mo-S systems. *Phys. Rev. B Condens. Matter Mater. Phys.* **79** (2009).
37. D.W. Brenner et al., A second-generation reactive empirical bond order (REBO) potential energy expression for hydrocarbons. J. Phys. Condens. Matter (2002). https://doi.org/10.1088/0953-8984/14/4/312
38. J.A. Stewart, D.E. Spearot, Atomistic simulations of nanoindentation on the basal plane of crystalline molybdenum disulfide (MoS2). Model. Simul. Mater. Sci. Eng. **21**, 45003 (2013)
39. N. Wakabayashi, H.G. Smith, R.M. Nicklow, Lattice dynamics of hexagonal MoS_2 studied by neutron scattering. Phys. Rev. B **12**, 659–663 (1975)
40. E. Cadelano, P. Palla, S. Giordano, L. Colombo, Nonlinear elasticity of monolayer graphene. Phys. Rev. Lett. **102**, 235502 (2009)
41. J.-S. Wang, B.K. Agarwalla, H. Li, J. Thingna, Nonequilibrium Green's function method for quantum thermal transport. Front. Phys. **9**, 673–697 (2014)
42. T. Eknapakul et al., Electronic structure of a quasi-freestanding MoS2 monolayer. Nano Lett. **14**, 1312–1316 (2014)
43. X. Zhang et al., Raman spectroscopy of shear and layer breathing modes in multilayer MoS2. Phys. Rev. B **87**, 115413 (2013)
44. R. Chen, J. Luo, D. Guo, X. Lu, Energy transfer under impact load studied by molecular dynamics simulation. J. Nanoparticle Res. **11**, 589–600 (2009)
45. M. Henkel, H.M. Urbassek, Ta cluster bombardment of graphite: molecular dynamics study of penetration and damage. Nucl. Instrum. Methods Phys. Res. Sect. B Beam Interact. Mater. Atoms **145**, 503–508 (1998)
46. S. Plimpton, Fast parallel algorithms for short-range molecular dynamics. J. Comput. Phys. **117**, 1–19 (1995)
47. A. Stukowski, Visualization and analysis of atomistic simulation data with OVITO–the open visualization tool. Model. Simul. Mater. Sci. Eng. **18**, 015012 (2009)
48. A. Ostadhossein et al., ReaxFF reactive force-field study of molybdenum disulfide (MoS2). J. Phys. Chem. Lett. **8**, 631–640 (2017)